Computers and Electronics in Agriculture 127 (2016) 699–707

Contents lists available at ScienceDirect

Computers and Electronics in Agriculture

journal homepage: www.elsevier.com/locate/compag

Original papers

Operational assessment of aboveground tree volume and biomass by terrestrial laser scanning

Konstantin Olschofsky, Volker Mues, Michael Köhl *

University of Hamburg, World Forestry, Leuschnerstrasse 91, 21031 Hamburg, Germany

ARTICLE INFO

Article history:
Received 3 March 2016
Received in revised form 25 July 2016
Accepted 28 July 2016
Available online 8 August 2016

Keywords:
Terrestrial laser scanning
Aboveground tree biomass
Occlusion
Allometric functions

ABSTRACT

The assessment of aboveground tree biomass (AGB) is essential to the evaluation of tree populations in forests, open landscapes, and urban areas. The predominant method used to determine AGB relies on error-prone functions derived from the statistical relationships of tree attributes and biomass. Terrestrial laser scanning (TLS) offers a new approach that replaces statistical AGB estimates with consistent measurements.

Aboveground tree biomass (AGB) comprises stems and branches. While the biomass assessment of stems is straightforward, TLS measurements of tree crowns are far more complex because of branch overlapping. Because placing reflecting targets in the crowns of tall standing trees is impractical, yet necessary for merging the point clouds from different laser scan positions, TLS measurements often fail in operational applications.

This study introduces a straightforward algorithm that simplifies biomass measurements of complex branch geometries using TLS and derives AGB by averaging measurements from individual scanning positions. We verified our approach through an experimental setup of branching systems with different complexities and known true biomass volumes. The results show that biomass extraction from branches by TLS systems is not affected by scanning distance. The combination of biomass measurements from individual scanning positions by averaging provides reliable biomass figures. Compared to the known true biomass figures, the overall accuracies achieved by our approach are 95% or higher, which brings the operational application of TLS for AGB measurements within tangible reach.

1. Introduction

Forests resource assessments collect a multitude of attributes that provide information on ecosystem functions, including timber production, biodiversity, health and vitality, or protective functions. Only a few attributes can be directly assessed by measurements (e.g. stem diameters, tree height) or visual observations (e.g. tree species, stem damage). These attributes provide input parameters for models or functions used to determine additional information. A widely known example is the estimation of stem volume based on allometric models using stem diameters and tree height as input parameters (Schreuder et al., 1992; Hush et al., 2003; Köhl et al., 2006). Because volume functions provide only an approximation to the true volume, they are prone to prediction errors (Gertner, 1984; McRoberts and Westfall, 2013). The problem of model prediction errors is further compounded when estimating the AGB of individual trees. While volume is a cubic measure (e.g. m^3), AGB is generally presented as a weight measurement (e.g. kg). AGB is obtained by either multiplying tree volume by wood density or by allometric biomass equations, which use tree attributes such as stem diameters or tree height as input variables (IPCC, 2003, 2006). Chave et al. (2004) state sources of errors associated with the estimation of AGB by means of allometric biomass equations, among which are errors due to tree measurement and errors due to the choice of an allometric model relating AGB to other tree dimensions. They found the choice of the allometric model to be the major source for errors.

According to Newnham et al. (2015) Terrestrial Laser Scanning (TLS) "presents an opportunity to go beyond simple empirical isometric and allometric equations to the point where three-dimensional measurements ... are used as a basis for assessing volume, ...". This statement is of particular significance considering the increasing importance of ABG assessments in forest carbon stock inventories (IPCC, 2003, 2006). TLS provides point clouds that can be used for geometrical modeling.

In our study we focus on the assessment of ABG with a special reference to measuring tree crown volumes, which has an even

* Corresponding author.
E-mail address: michael.koehl@uni-hamburg.de (M. Köhl).

http://dx.doi.org/10.1016/j.compag.2016.07.030
0168-1699/

greater margin of error than measuring tree stem volumes. We utilize an experimental setup of different branching patterns. The true volume of branches was assessed by water displacement. We develop a straightforward algorithm for the extraction of branch volumes in individual scans. Theoretically, TLS could potentially be an ideal tool for assessing the complex geometrical structures of tree crowns. In practice, however, the occlusion of branches presents a major obstacle for the geometrical modeling of tree crowns. The problem of occlusion can be minimized when scans from multiple scan locations are merged into a single point cloud. This approach uses highly reflective targets that can be observed from the multiple scan locations. In practical applications the positioning of targets in tall tree crowns can be cumbersome, as they in turn may be subject to occlusion. Therefore, Henning and Radtke (2006) consider the use of reflective targets in forest applications to be impractical. Instead of merging scans into one point cloud we use the mean of volumes extracted from individual scans to provide an estimate of the total volume.

1.1. TLS measurements for tree volume and biomass assessments

Terrestrial laser scanners measure the relative position of laser beam reflecting objects. In addition to the reflection intensity, scanners record the reflection's position using polar coordinates based on horizontal angle, vertical angle, and the object distance. Distances can be measured either by the concept of (1) time of flight or the (2) range distances approach. While a time of flight scanner derives the distance from the time period between signal emission and the detection of the reflected signal, range distance scanners use the phase shift of a permanent emitted laser beam. Systems working with the range distance approach can detect various reflections from the first to the last palls. These are mainly used for airborne laser scanning. Most terrestrial laser scanners use the time of flight concept, whereby each point has one return and one distinct measured coordinate (Danson et al., 2014).

Different approaches are described for the analysis of point clouds from TLS systems. The general idea behind TLS analyses is the transfer of point clouds into geometric objects, which is realized through geometric modeling. Another approach is voxelation (Hosoi et al., 2013; Fernández-Sarría et al., 2013), which combines clusters of points into cubes, i.e. 3D-pixels, of defined size. A third approach is point cloud meshing (Kazhdan et al., 2006), which approximates a given volume by an entity of small and simple objects. Nölke et al. (2015) used this approach to measure the volume of plank buttressed tropical trees. A major obstacle in analyzing TLS clouds is occlusion. From a scanner position occlusion is caused by objects that cast shadows and thus hide background objects from detection. Combining points clouds from multiple scan positions into one common cloud can partly solve the problem of occlusion (Hilker and Coops, 2012).

Xu et al. (2013) compared different methods for tree crown projections and crown volume estimations for a virtual set of 22 common tree species in China derived by TLS. He showed how the different methods influenced the estimation accuracy, whereby the potential of estimation of branch and twigs structures was excluded.

In forestry applications the analysis of TLS mainly focuses on the extraction of attributes from point clouds that are traditionally used in terrestrial forest surveys, such as stem diameters, height, or number of trees (Dassot et al., 2012). The estimation of standing timber volume based on TLS data has been described by Hopkinson et al. (2004), who extracted stem diameter and tree height from laser point clouds and used those as input variables for allometric timber volume functions. Aschoff and Spiecker (2004) used TLS-derived stem diameters at 1.3 m and 7 m, which are frequently used input variables for volume functions in Europe (Kaufmann, 2002; Tomppo et al., 2010). Taper functions, which are a recognized alternative for the assessment of stem volumes (Kublin and Breidenbach, 2013; Kublin et al., 2013), were extracted from TLS by Maas et al. (2008). Further applications of TLS for assessing tree height, diameter at breast height (DBH), stem density, canopy cover, and AGB are presented by (Hopkinson et al., 2004; Bienert et al., 2006; Kankare et al., 2013). In addition, TLS has been used to estimate leaf area(Huang and Pretzsch, 2010) sweep and lean (Thies et al., 2004), tree value (Murphy et al., 2010), fibre quality (van Leeuwen et al., 2011), forest canopy structures (Parker et al., 2004) or fuelwood quantity (Loudermilk et al., 2007).

Nölke et al. (2015) are among the few who do not limit the analysis of TLS point clouds to the extraction of individual tree attributes, but use the entire point cloud for measuring volumes of tree buttresses. As tree buttresses are solid objects the problem of occlusion can be solved by merging the point clouds assessed from multiple scan positions. This precondition does not hold true for tree crowns, where overlapping of branch structures frequently occurs. This is a crucial issue for the estimation of AGB, as a considerable proportion of aboveground biomass is located in tree crowns and not in the stem (Otto, 1994; Burschel and Huss, 2003). Because the assessment of stem volume is generally more accurate than the assessment of tree crowns, the total error of AGB assessments is substantially driven by the uncertainties related to tree crown assessments. Therefore, methods for improving the reliability of the assessment of tree crown volume are of uttermost importance.

2. Material and methods

Branches originating from the crowns of Sessile oak trees (*Quercus petraea*) are the objects of our study. Three to four meter long branches were collected from logging residuals after harvesting operations in a sustainably managed oak stand near Reinbek, Germany (53°31′N, 10°16′E). Due to microclimate of the forest, some of the branches were lichened. We systematically arranged branch segments for a terrestrial laser scanning under standardized laboratory conditions which allowed for an exact assessment of biomass and volume of the scanned objects. To ensure standard conditions, we used a reference cube with a fixed side length (of 540 mm) the outlines of which determine the biomass which has to be assessed in different ways. Any twigs protruding from the surface of the cube were cut back to the cube's boundary.

2.1. Experimental setup

While Hildebrandt and Iost (2012) studied the applicability of laser scanning for tree volume estimation by utilizing regular, artificial bodies, we choose an approach that provides for the variability of tree crowns caused by different patterns of branch structure and branch size. Branches of Sessile oak (*Quercus petraea*) were collected before foliation and arranged in a $50 * 50 * 50$ cm reference cube (Fig. 1). In 19 different experimental setups the reference

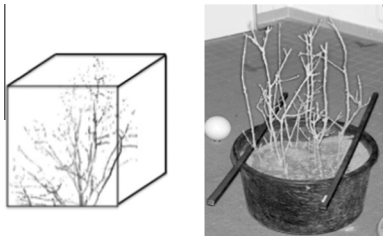

Fig. 1. Schematic sketch (left) and sample image (right) of the reference cube filled with branches.

cube was filled with branches of varying size and branching structure (Fig. 2). For each setup the volume was measured by fluid displacement (measuring accuracy 5 ml).

For each of the 19 experimental setups laser scans were taken from three different positions with three different resolutions (25%, 50% and 100% from 19 Laser beams per angular degree). The resolutions can be regarded as proxies for different measurement distances in in-situ assessments (i.e. 2.5 m, 5 m, and 10 m) (Fig. 3). For each of the 19 experimental setups, 9 laser scans (3 resolutions $*$ 3 positions) were assessed resulting in a total of 171 scans. The branch arrangements in the 19 cubes are shown in Fig. 2.

We used the Faro Focus 3D 120 Laser Scanner, which assesses objects in the range form 0.6 m to 120 m using the phase-shift principle. The margin of error in 25 m distance is less than 2 mm. The applied Faro scanner is practical for operational applications in forest inventories, as it is very light (5 kg), scans up to 976.000 points per second, includes a color camera, GPS, compass, and height sensor, is remote controlled and can be connected to the internet.

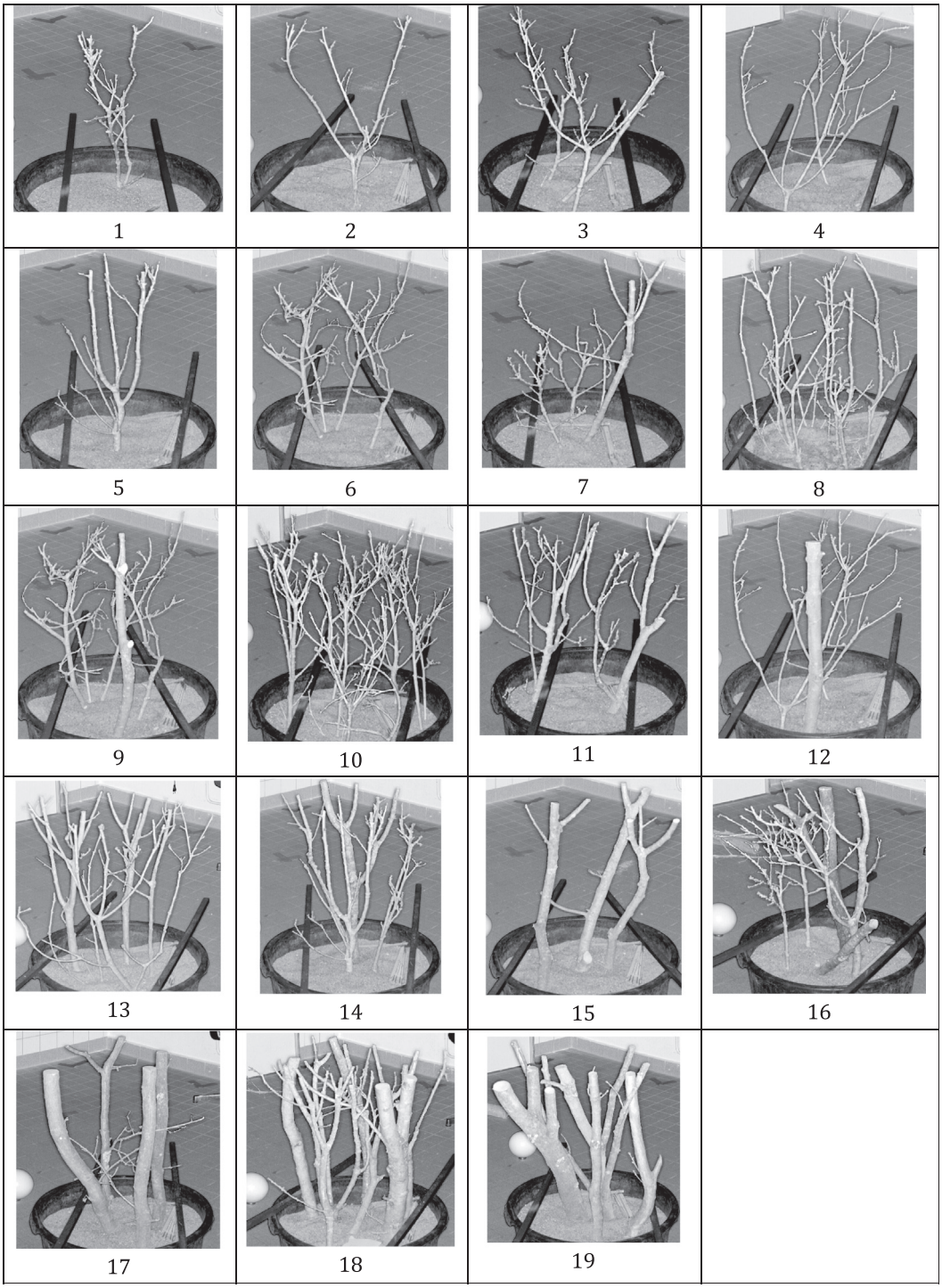

Fig. 2. 19 branch arrangements in the reference cube.

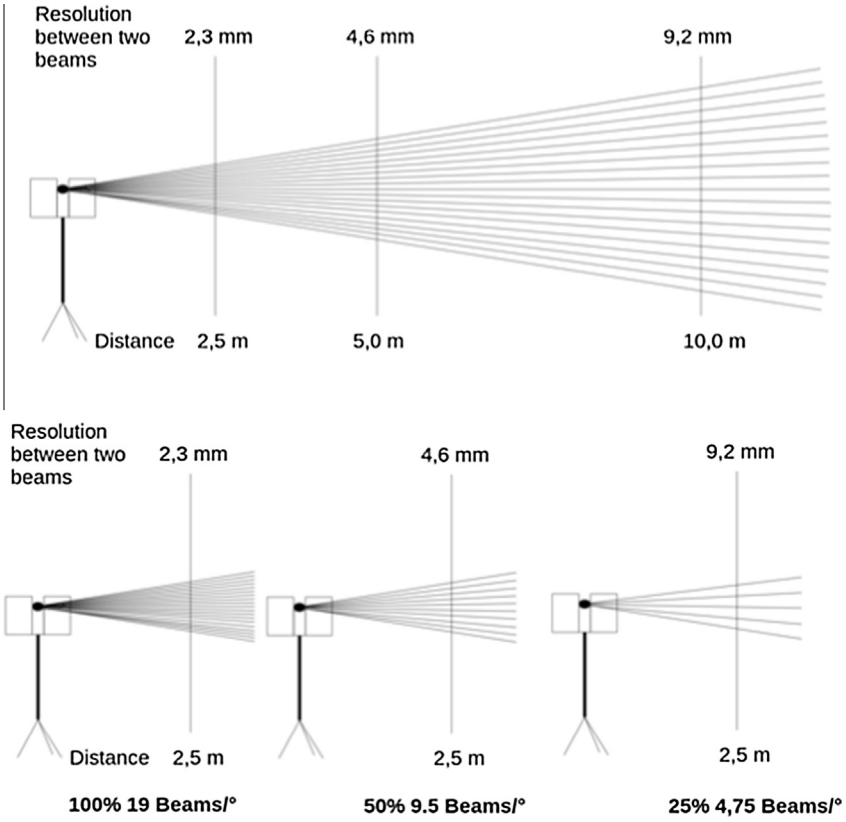

Fig. 3. Relation between object distance and beam distance. Top: 19 Beams per Degree. Bottom: 100%, 50% and 25% beam distance in 2.5 m object distance.

The difference between laser-based volume measurements from true volumes was tested for statistical significance by two-sided paired *t*-Tests with significance level of $\alpha = 0.05$.

2.2. Evaluation algorithm

To analyze the laser scans we developed a special evaluation algorithm that allows for the identification of branches and subsequent assessment of the woody biomass. The evaluation algorithm uses 7 subsequent steps.

2.2.1. Step 1: Separation of the reference cube from surrounding environment

Laser scanning captures the entire environment and extends beyond the objects of interest. For our analyses, objects outside the reference cube had to be eliminated. As the reference cube constitutes a 3-dimensional body, manual delineation was found to be the most straightforward method for separating the cube from the environment. However, manual delineation is only a viable procedure in experimental setups. In practical applications automated procedures are preferred.

2.2.2. Step 2: Elimination of outliers

Each scan includes outlier artifacts that do not provide any specific information on the objects to be assessed. A filter was applied that uses two approaches for eliminating outliers. Firstly, outliers were identified with respect to the intensity of reflection. Measurements below a threshold of 13% of total reflecting intensity are excluded from further analyses. Secondly, spatial boundaries were applied to exclude any outliers. The distance to the nearest adjacent points was calculated for each laser point. Where the distance was larger than a threshold value, the respective laser point was eliminated (Fig. 4).

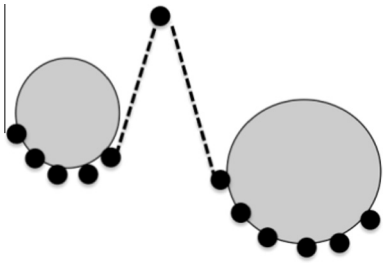

Fig. 4. Distance threshold for eliminating outliers (dotted lines indicate distances between points above a threshold values).

2.2.3. Step 3: Identification of branches

Along the direction of horizontal lines adjacent laser points were identified and the length of the line segments was used as an indicator for the diameter of branches (Fig. 5).

2.2.4. Step 4: Separation of branches

Where two branches are slightly offset to the side, step 3 treats them as one branch and fails to separate them, as only the distance

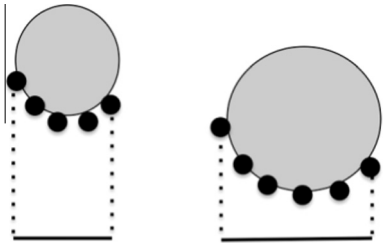

Fig. 5. Identification of branch diameters.

along the x-direction is considered. Therefore, the distance, y, of points with reference to the scanner was used to separate those branches. Where the distance in y-direction indicated a fissure, a separator in x-direction was used to differentiate two branches (Fig. 6).

2.2.5. Step 5: Construction of discs

For each branch the distance between the first and last hit in x-direction was taken as a measure for the diameter, d_i, of a branch (see Fig. 7). Given the large number of observations, it is assumed that elliptical abnormalities are cancelled out and the diameter is an appropriate measure to calculate the disc area of the stem, A_i, by

$$A_i = \frac{\pi}{4} d_i^2$$

2.2.6. Step 6: Volume estimation

The calculation of branch volumes uses cylinders that are constructed for each of the discs identified in the previous step. The distance between individual discs is taken as an approximation for the length of the individual cylinders and is obtained by the functional relationship between vertical viewing angle, distance between scanner and object, and scanner resolution. The vertical distances between adjacent discs, d_{vi}, were used to expand the disc areas A_i to the volume of the respective cylinders, V_i, (Fig. 8) by aggregating the volumes of individual cylinders, V_i, gives the total biomass volume.

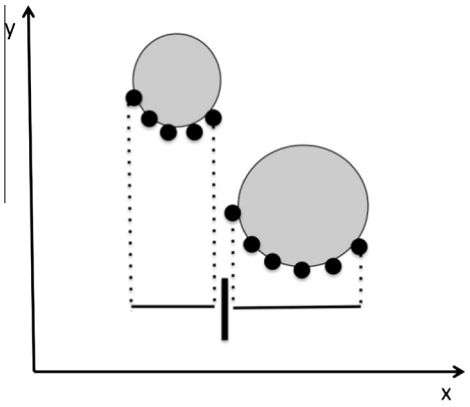

Fig. 6. Separation of branches slightly offset to the side; illustration of x- and y-axis.

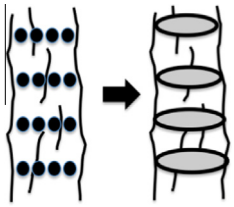

Fig. 7. Deriving discs (right) from hits (left).

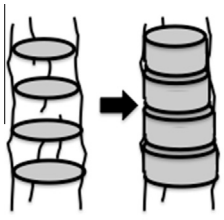

$V_i = A_i * d_{Vi}$

where
V_i = volume of cylinder i
A_i = area of disc i
d_{vi} = mean vertical distance between disc i adjacent discs

$$= \frac{d_{Vi-1} + d_{Vi+1}}{2}$$

Fig. 8. Deriving cylinder volumes (right) by utilizing vertical distances between discs (left).

2.2.7. Step 7: Biomass estimation

Conversion from volume to biomass requires information on the branch density. The given example uses branches exclusively from Sessile oak tree crowns and assumes a constant density.

3. Results

The volume of branches of the individual 19 cubes assessed by water displacement is presented in Table 2. These volumes are further referred to as true volumes. Volumes range from 90.4 cm^3 to 4435.5 cm^3.

For each cube, measurements are taken from three viewing positions in coarse, medium, and fine resolution, resulting in a total of 171 measurements. Fig. 9 presents the laser scanning point clouds of one viewing point obtained for three different resolutions for cube 1.

The volume was calculated independently for each measurement. Table 1 shows the absolute values and the percent difference from the corresponding true value. The differences of measured volumes from true volumes range from −34.3% (cube 9, fine resolution) to +36.75% (cube 3, coarse resolution). Out of the 171 measurements, 65 (38%) show a difference from the true volume of less than ±5%. In six cubes the measurements result in consistently smaller volumes than the true volume (cube 2, 8, 10, 13, 14, 18), in cube 3 almost all measurements overestimate the true volume. In all other cubes both, positive and negative differences are observed.

The 171 cell values presented in Table 1 were derived independently for each position and resolution. The algorithm applied did not use a geometric merge of point clouds from the different positions. For each cube and each resolution the mean volume of individual volume measurements from the three positions was calculated. The resulting 57 mean volumes (19 cubes times 3 resolutions) are presented in Table 1.

The relative differences between true and mean TLS measured volumes range from −14.3% (cube 2, fine resolution) to +17.2% (cube 3, medium resolution). Differences between resolutions are not significant (paired *t*-Test, 2-sided, $\alpha = 0.05$). The overall mean accuracies for all 19 cubes amount to 97.1% (coarse resolution), 96.5% (medium resolution), and 95% (fine resolution).

Noticeable differences of TLS measurements from true values are found for three cubes. In cubes 2 and 4, TLS measurements are consistently lower than true volumes (−14.3% to −9.6%), while in cube 3 all TLS measurements result in larger volumes (+13% to +17.2%). A possible explanation for these differences is the geometric pattern of branches. Cubes 2 and 4 have a comparably high frequency of branch forks. At a branch fork the cross sectional area of a stem takes on an oval shape. Under the general assumption of circular cross sections of branches oval branch forks calculations may lead to larger volumes. In cube 3 two or more branches overlap in all viewing positions, which results in lower volumes.

Table 1
True volume of the individual 19 cubes assessed by water displacement, and coarse, medium, and fine TLS resolution (values in brackets are TLS volumes in %- of true value).

		Volume [cm^3]								
			TLS								
	Branch setup		Coarse			Medium			Fine		
Cube		True volume	Pos. 1	Pos. 2	Pos. 3	Pos. 1	Pos. 2	Pos. 3	Pos. 1	Pos. 2	Pos. 3
1	2 thin branches	90.4	94.0	94.0	72.3	94.1	95.6	76.9	89.5	93.9	86.0
	1 thin branch		(104.1)	(104.0)	(80.0)	(104.1)	(105.7)	(85.0)	(99.0	(103.8)	(95.2)
2	3 thin branches	100.6	87.0	92.7	93.2	88.4	84.7	96.5	85.9	81.5	91.4
	2 thin branches		(86.4)	(92.1)	(92.6)	(87.9)	(84.2)	(95.8)	(85.4)	(81.0)	(90.8)
3	1 medium branch	158.6	152.4	216.8	173.5	176.6	184.4	196.7	184.7	168.3	185.0
	4 thin branches		(96.1)	(136.7)	(109.4)	(111.3)	(116.2)	(124.0)	(116.4)	(106.1)	(116.6)
4	1 medium 2 thin branches	160.8	127.2	145.9	143.5	122.5	149.4	159.1	124.7	144.9	157.1
	Thin branches covered with buds		(79.1)	(90.8)	(89.2)	(76.2)	(92.9)	(98.9)	(77.6)	(90.1)	(97.7)
5	4 thin branches (set 6) + one medium branch	216.1	215.7	195.4	227.8	209.8	159.2	222.5	206.6	194.9	219.7
	Many thin branches		(99.8)	(90.4)	(105.4	(97.1)	(73.7	(103.0)	(95.6)	(90.2)	(101.6)
6	1 medium and 3 thin branches	270.0	246.3	341.9	290.6	266.5	339.5	299.5	272.1	321.6	321.8
	2 thin (set 4) plus one thick branches		(91.2)	(126.7)	(107.6	(98.7)	(125.7	(110.9)	(100.8)	(119.1)	(119.2)
7	Many small branches	295.1	257.2	375.7	260.2	287.5	312.7	269.0	302.3	302.5	271.7
	1 medium (set 5) and 2 thin branches		(87.2)	(127.3)	(88.2	(97.4)	(106.0	(91.2)	(102.5)	(102.5)	(92.1)
8	3 middle sized branches	329.1	300.4	321.6	321.0	308.5	276.1	326.7	303.0	278.9	316.5
	stuffed with mixed of branches		(91.3)	(97.7)	(97.5	(93.7)	(83.9	(99.3)	(92.0)	(84.7)	(96.2)
9	Thick branches	527.1	429.2	607.9	545.1	425.4	538.6	537.7	346.1	543.0	547.1
	Mix of medium and small branches		(81.4)	(115.3)	(103.4	(80.7)	(102.2	(102.0)	(65.7)	(103.0)	(103.8)
10	Thick branches	527.9	469.0	515.7	493.1	492.1	497.2	504.4	463.9	465.8	501.8
	2 thin branches		(88.8)	(97.7)	(93.4	(93.2)	(94.2	(95.5)	(87.9)	(88.2)	(95.0)
11	1 thin branch	551.9	530.4	453.7	521.3	569.5	446.5	543.5	514.8	435.8	539.2
	3 thin branches		(96.1)	(82.2)	(94.5	(103.2)	(80.9	(98.5)	(93.3)	(79.0)	(97.7)
12	2 thin branches	684.5	555.3	746.7	716.5	560.1	714.7	711.0	548.0	697.9	702.4
	1 medium branch		(81.1)	(109.1)	(104.7	(81.8)	(104.4	(103.9)	(80.0)	(102.0)	(102.6)
13	4 thin branches	857.0	810.6	703.0	753.7	810.9	705.5	786.0	792.5	695.7	749.5
	1 medium 2 thin branches		(94.6)	(82.0)	(87.9	(94.6)	(82.3	(91.7)	(92.5)	(81.2)	(87.4)
14	Thin branches covered with buds	932.2	903.6	884.9	797.2	925.0	806.7	806.6	874.0	801.5	771.1
	4 thin branches (set 6) + one medium branch		(96.9)	(94.9)	(85.5	(99.2)	(86.5	(86.5)	(93.7)	(86.0)	(82.7)
15	Many thin branches	1127.7	1181.0	1108.0	1302.9	1162.8	1144.5	1322.1	1161.9	1159.5	1318.1
	1 medium and 3 thin branches		(104.7)	(98.2)	(115.5	(103.1)	(101.5	(117.2)	(103.0)	(102.8)	(116.9)
16	2 thin (set 4) plus one thick branches	1507.6	1519.0	1471.7	1331.2	1530.6	1405.7	1330.6	1532.2	1401.9	1367.9
	Many small branches		(100.8)	(97.6)	(88.3	(101.5)	(93.2	(88.3)	(101.6)	(93.0)	(90.7)
17	1 medium (set 5) and 2 thin branches	2674.4	2682.5	2569.3	2872.2	2586.3	2418.5	2814.6	2564.6	2427.0	2771.0
	3 medium branches		(100.3)	(96.1)	(107.4	(96.7)	(90.4	(105.2)	(95.9)	(90.7)	(103.6)
18	Many mixed branches	3917.9	3277.0	3883.7	3429.1	3302.2	3906.8	3426.9	3210.9	3839.9	3340.3
	Thick braches		(83.6)	(99.1)	(87.5	(84.3)	(99.7	(87.5)	(82.0)	(98.0)	(85.3)
19	Mix of medium and small branches	4435.5	4475.7	4412.6	4204.7	4281.6	4314.8	4168.9	4080.7	4009.7	4139.4
	Thick branches		(100.9)	(99.5)	(94.8	(96.5)	(97.3	(94.0)	(92.0)	(90.4)	(93.3)

Table 2
True volume of the individual 19 cubes and volume by cube and resolution.

	True volume [cm^3]	Resolution					
		Coarse		Medium		Fine	
Cube		Volume [cm^3]	Difference compared to true volume [%]	Volume [cm^3]	Difference compared to true volume [%]	Volume [cm^3]	Difference compared to true volume [%]
1	90.4	86.8	−4	88.8	−1.7	89.8	−0.7
2	100.6	91.0	−9.6	89.9	−10.7	86.3	−14.3
3	158.6	180.9	+14.0	185.9	+17.2	179.3	+13.0
4	160.8	138.9	−3.6	143.7	−10.7	142.2	−11.5
5	216.1	213.0	−1.5	197.2	−8.8	207.0	−4.2
6	270.0	292.9	+8.5	301.8	+11.8	305.2	+13.0
7	295.1	297.7	+0.9	289.7	−1.8	292.2	−1.0
8	329.1	314.4	−4.5	303.8	−7.7	299.5	−9.0
9	527.1	527.4	+0.1	500.6	−5.0	478.7	−9.2
10	527.9	492.6	−6.7	497.9	−5.7	477.1	−9.6
11	551.9	501.8	−9.1	519.8	−5.8	496.6	−10.0
12	684.5	672.8	−1.7	661.9	−3.3	649.4	−5.1
13	857.0	755.7	−11.8	767.5	−10.5	745.9	−13.0
14	932.2	861.9	−7.5	846.1	−9.2	815.5	−12.5
15	1127.7	1197.3	+6.2	1209.8	+7.3	1213.2	+7.6
16	1507.6	1440.7	−4.4	1422.3	−5.7	1434.0	−4.9
17	2674.4	2708.0	+1.3	2606.5	−2.5	2587.5	−3.2
18	3917.9	3529.9	9.9	3545.3	9.5	3463.7	−11.6
19	4435.5	4364.3	−1.6	4255.1	−4.1	4076.6	−8.1

Fig. 9. Laser scanning point clouds obtained for branch arrangements in cube 1 (2 thin branches) for coarse (left), medium (middle), and fine (right) resolution.

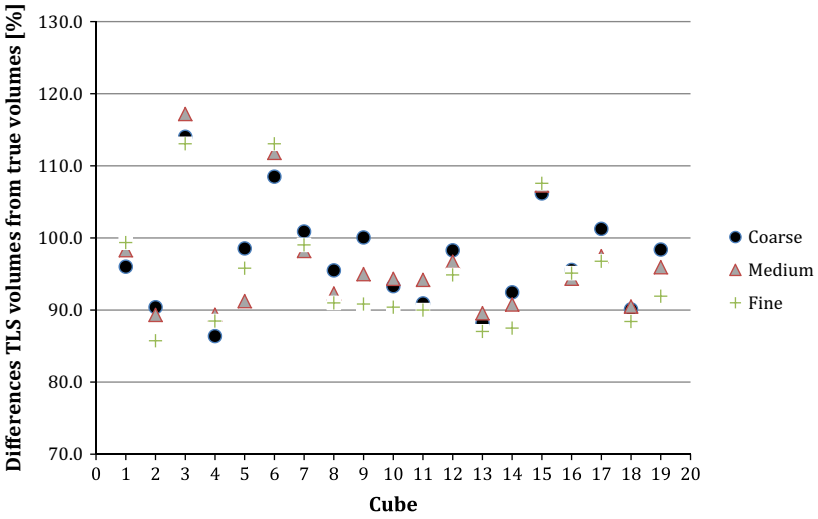

Fig. 10. Percent differences of TLS measured volumes from true values (100%).

The individual percent differences of TLS measured volumes from true values are presented in Fig. 10. The plotted values show that differences are affected by cubes and not by the TLS resolution. This suggests that the geometry of branch arrangements provide reasonable grounds for the observed differences. The geometry of branch arrangements results in different frequencies of occlusion and deviations from circular cross sections.

The three resolutions do not show a uniform sequence of differences from true volumes, which is another indication of the dependency of TLS volume measurement accuracies on the geometry of branch arrangements.

4. Discussion

In our approach each laser scan is treated independently. Individual volume measurements from different viewing positions are combined by the straightforward calculation of a mean value. This simplified approach abandons the spatial consolidation of laser measurements from different viewing positions and thus is not subject to errors introduced by complex geometric calculations and does not require the (impractical) installation of targets at large heights. However, the advantage of introducing simplicity is achieved at the cost of errors due to overlapping branches.

Our results show that the simplified approach results in overall accuracies of 95% or better. Individual differences of measured volumes from true volumes range from −14.3% to +17.2%. It is important to emphasize that these results were obtained for complex geometric patterns of branch arrangements, which are often found under realistic conditions.

No significant differences could be found between resolutions. The frequency of hits is found not to be decisive for the obtained accuracies. In addition, the resolutions applied can be considered as a proxy for different distances between a laser scanner and the observed object. Therefore, we show that measurements do not depend on measurement distances, at least up to a maximum threshold that is defined by the distance between adjacent laser beams and the diameter of branches. Where distances between laser beams become larger than the diameter of branches, individual branches may not contribute to the reflection of laser beams. However, our results provide evidence for the operational applicability of TLS for the measurement of tree crown biomass. Under operational conditions the distances between laser instruments and the targeted branches will vary due to the length of tree crowns. Our results suggest that measurements in different tree crown heights are operationally feasible.

The accuracy of our results has to be studied in the light of currently applied methods for the estimation of tree biomass. A generally applied approach is the application of tree biomass functions (Chave et al., 2005; Zianis et al., 2005; IPCC, 2006; Köhl et al., 2015). Biomass functions use measurements of tree attributes such as tree height, stem diameters or crown length to estimate the aboveground biomass of trees. Despite their wide use, biomass functions result in substantial errors, mainly due to the heterogeneous and complex geometric patterns of tree crowns (Chave et al., 2004; Case and Hall, 2008; Domke et al., 2012; McRoberts and Westfall, 2013; Breidenbach et al., 2014). Errors associated with the application of tree biomass functions are generally larger than five percent. A substantial part of tree biomass is located in the tree stem, and its volume can be reliably estimated by the application of geometric solids (Köhl et al., 2006). Thus, a substantial share of the total error associated with the application of aboveground tree biomass functions is introduced by the estimation of

tree crown biomass. Because our study concentrates only on branch arrangements that reflect tree crowns, there is evidence that the overall error in measuring total aboveground tree biomass (i.e. tree crown and stem) by TLS is substantially lower than errors associated to biomass estimation by tree biomass functions.

5. Conclusions

The aboveground biomass (AGB) of trees is crucial information for initiatives such as bio-economy, renewable energy, or climate change mitigation, which are high on the political agenda. Yet, contrary to its societal and environmental importance, the current assessment of AGB is burdened with substantial uncertainty (Monni et al., 2007). Existing practices in AGB assessments apply functional relationships of measurable tree attributes (e.g. stem diameter, tree height, crown length, crown diameter) with AGB, and often fail to include the large natural variability of individual tree branch geometries and related biomass of tree crowns. Therefore, it has long been a goal to replace individual tree AGB estimates with reliable measurements.

TLS makes individual tree AGB measurements potentially possible. A major obstacle is the complex structure of branches in tree crowns that lead to overlapping in the visual field. A classical TLS approach would address this issue by combining scans from different points of view, which would require installing reflecting targets in order to merge individual TLS scans. In extensive operational surveys, the installation of targets in tall tree crowns is impractical given the extreme heights, which can easily exceed 20 m above ground.

We present an approach that brings the operational application of TLS for AGB measurements within tangible reach. We show that biomass extraction by TLS systems is not affected by scanning distance. A straightforward algorithm is presented that simplifies AGB measurements of complex branch geometries. By taking the average of AGB measurements from individual scan positions, the installation of targets in difficult to reach heights can be avoided. The presented approach is certainly still prone to errors; however, the resulting uncertainties are substantially smaller than those of currently applied methods that are based on statistical relationships between tree attributes and AGB. This offers an arena for new inventory approaches for extensive biomass assessments especially in the scope of the Framework Convention on Climate Change (UN-FCCC) such as carbon stock assessments, greenhouse gas inventories, or measurement, reporting and verification (MRV) under REDD + (Reducing Emissions from Deforestation and Forest Degradation) schemes.

Acknowledgement

This study was technical partially supported by the German Ministry for Food and Agriculture. The authors thank Dr. Dierk Kownatzki for supporting the concept, the measurements and data pre-processing. We are grateful for the valuable comments of two anonymous reviewers that helped to improve the first version of the manuscript.

References

Aschoff, T., Spiecker, H., 2004. Algorithms for the automatic detection of trees in laser scanner data. Int. Arch. Photogramm., Remote Sens. Spat. Informat. Sci. 36, 71–75.

Bienert, A., Scheller, S., Keane, E., Mullooly, G., Mohan, F., 2006. Application of terrestrial laser scanners for the determination of forest inventory parameters. In: Proceedings of the International Archives of Photogrammetry. Remote Sensing and Spatial Information Sciences, Dresden, Germany.

Breidenbach, J., Antón-Fernández, C., Petersson, H., McRoberts, R.E., Astrup, R., 2014. Quantifying the model-related variability of biomass stock and change estimates in the norwegian national forest inventory. For. Sci. 60, 25–33.

Burschel, P., Huss, J., 2003. Grundriss des Waldbaus. Ulmer Suttgart.

Case, B.S., Hall, R.J., 2008. Assessing prediction errors of generalized tree biomass and volume equations for the boreal forest region of west-central Canada. Can. J. For. Res. 38, 878–889.

Chave, J., Andalo, C., Brown, S., Cairns, M.A., Chambers, J.Q., Eamus, D., Fölster, H., Fromard, F., Higuchi, N., Kira, T., Lescure, J.-P., Nelson, B.W., Ogawa, H., Puig, H., Riéra, B., Yamakura, T., 2005. Tree allometry and improved estimation of carbon stocks and balance in tropical forests. Oecologia 145, 87–99.

Chave, J., Condit, R., Aguilar, S., Hernandez, A., Lao, S., Perez, R., 2004. Error propagation and scaling for tropical forest biomass estimates. Philosoph. Transact. Roy. Soc. Lond. 359, 409–420.

Danson, F.M., Gaulton, R., Armitage, R.P., Disney, M., Gunawan, O., Lewis, P., Pearson, G., Ramirez, A.F., 2014. Developing a dual-wavelength full-waveform terrestrial laser scanner to characterize forest canopy structure. Agric. For. Meteorol. 198–199, 7–14.

Dassot, M., Colin, A., Santenoise, P., Fournier, M., Constant, T., 2012. Terrestrial laser scanning for measuring the solid wood volume, including branches, of adult standing trees in the forest environment. Comput. Electron. Agricult. 89, 86–93. http://dx.doi.org/10.1016/j.compag.2012.08.005.

Domke, G.M., Woodall, C.W., Smith, J.E., Westfall, J.A., McRoberts, R.E., 2012. Consequences of alternative tree-level biomass estimation procedures on U.S. forest carbon stock estimates. For. Ecol. Manage. 270, 108–116.

Fernández-Sarría, A., Velázquez-Martí, B., Sajdak, M., Martínez, L., Estornell, J., 2013. Residual biomass calculation from individual tree architecture using terrestrial laser scanner and ground-level measurements. Comput. Electron. Agricult. 93, 90–97. http://dx.doi.org/10.1016/j.compag.2013.01.012.

Gertner, G.Z., 1984. The sensitivity of measurement error in stand volume estimations. Can. J. For. Res. 16, 1120–1123.

Henning, J., Radtke, P., 2006. Detailed stem measurements of standing trees from ground-based scanning lidar. For. Sci. 52, 67–80.

Hildebrandt, R., Iost, A., 2012. From points to numbers: a database-driven approach to convert terrestrial LiDAR point clouds to tree volumes. Eur. J. For. Res. 131, 1857–1867.

Hilker, T., Coops, N., 2012. A simple technique for co-registration of terrestrial LiDAR observations for forestry applications. Remote Sens. Lett. 3, 239–247.

Hopkinson, C., Chasmer, L., Young-Pow, C., Treitz, P., 2004. Assessing forest metrics with a ground-based scanning LiDAR. Can. J. Remote Sens. 34, 573–583.

Hosoi, F., Nakai, Y., Omasa, K., 2013. 3-D voxel-based solid modeling of a broad-leaved tree for accurate volume estimation using portable scanning lidar. SPRS J. Photogramm. Remote Sens. 82, 41–48.

Huang, P., Pretzsch, H., 2010. Using terrestrial laser scanner for estimating leaf areas of individual trees in a conifer forest. Trees 24, 600–619.

Hush, B., Beers, T.W., Kershaw, J.A., 2003. Forest Mensuration. John Wiley & Sons, New York.

IPCC, 2003. Good Practice Guidance for Land Use, Land-use Change and Forestry. Institute for Global Environmental Strategies (IGES), Hayama, Japan.

IPCC, 2006. Agriculture, Forestry and other Land Use. In: Eggleston, S., Buendia, L., Miwa, K., Ngara, T., Tanabe, K. (Eds.), 2006 IPCC Guidelines for National Greenhouse Gas Inventories, vol. 4. Institute for Global Environmental Strategies, Hayama, Japan.

Kankare, V., Vastaranta, M., Holopainen, M., Raety, M., Yu, X., Hyyppa, J., Hyyppa, H., Alho, P., Viitala, R., 2013. Retrieval of forest aboveground biomass and stem volume with airborne scanning LiDAR. Remote Sens. 5, 2257–2274.

Kaufmann, E., 2002. Estimation of standing timber, growth and cut. In: Brassel, P., Lischke, H. (Eds.), Swiss National Forest Inventory: Methods and Models of the Second Assessment. Swiss Federal Research Institute WSL, Birmensdorf, Switzerland, pp. 162–196.

Kazhdan, M., Bolitho, M., Hoppe, H., 2006. Poisson surface reconstruction. In: Polthier, K., Sheffer, A. (Eds.), Proceedings of the "Eurographics Symposium on Geometry Processing", Cagliari (Italy).

Köhl, M., Lasco, R., Cifuentes, M., Jonsson, Ö., Korhonen, K.T., Mundhenk, P., de Jesus Navar, J., Stinson, G., 2015. Changes in forest production, biomass and carbon: results from the 2015 UN FAO Global Forest Resources Assessment. For. Ecol. Manage. 352, 21–34.

Köhl, M., Magnussen, S., Marchetti, M., 2006. Sampling Methods, Remote Sensing and GIS Multiresource Forest Inventory. Springer, Berlin, Heidelberg.

Kublin, E., Breidenbach, J., 2013. Package "TapeR". <https://cran.r-project.org/web/packages/TapeR/vignettes/TapeR.pdf> (access: 5.5.2016).

Kublin, E., Breidenbach, J., Kaendler, G., 2013. A flexible stem taper and volume prediction method based on mixed-effects B-spline regression. Eur. J. For. Res. 132, 983–997.

Loudermilk, E.L., Singhania, A., Fernandez, J.C., Hiers, J.K., O'Brien, J.J., Cropper Jr., W. P., Slatton, K.C., Mitchell, R.J., 2007. Application of ground-based lidar for fine-scale forest fuel modeling. In: Butler, Bret W.; Cook, Wayne, comps. (Eds.), The fire environment–innovations, management, and policy; conference proceedings, 26–30 March 2007, pp. 515–523.

Maas, H.-G., Bienert, A., Scheller, S., Keane, E., 2008. Automatic forest inventory parameter determination from terrestrial laser scanner data. Int. J. Remote Sens. 29, 1579–1593.

McRoberts, R.E., Westfall, J.A., 2013. Effects of uncertainty in model predictions of individual tree volume on large area volume estimates. For. Sci. 60, 34–43.

Murphy, G.E., Acuna, A.M., Dumbrell, I., 2010. Tree value and log product yield determination in Radiata pine (Pinus radiata) plantations in Australia: comparisons of terrestrial laser scanning with a forest inventory system and manual measurements. Can. J. For. Res. 40, 2223–2233.

Monni, S., Peltoniemi, M., Palosuo, T., Lehtonen, A., Mäkipää, R., Savolainen, I., 2007. Uncertainty of forest carbon stock changes – implications to the total uncertainty of GHG inventory of Finland. Climat. Change 81 (3), 391–413.

Newnham, G.J., Armston, J.D., Calders, K., Disney, M.I., Lovell, J.L., Schaaf, C.B., Strahler, A.H., Danson, F.M., 2015. Terrestrial laser scanning for plot-scale forest measurement. Curr. Forest. Rep. 1, 239–251.

Nölke, N., Fehrmann, L., I Nengah, S., Tiryana, T., Seidel, D., Kleinn, C., 2015. On the geometry and allometry of big-buttressed trees – a challenge for forest monitoring: new insights from 3D-modeling with terrestrial laser scanning. iForest – Biogeosci. Forest. 8, 574–581.

Otto, H.J., 1994. Waldökologie. Ulmer, Stuttgart.

Parker, G.G., Harding, D.J., Berger, M., 2004. A portable LIDAR system for rapid determination of forest canopy structure. J. Appl. Ecol. 41, 755–767.

Schreuder, H., Gregoire, T.G., Wood, G.B., 1992. Sampling Methods for Multiresource Forest Inventory. Wiley, New York.

Thies, M., Pfeifer, N., Winterhalder, D., Gorte, B.G.H., 2004. Three-dimensional reconstruction of stems for assessment of taper, sweep, and lean based on laser scanning of standing trees. Scand. J. For. Res. 19, 571–581.

Tomppo, E., Gschwantner, T., Lawrence, M., McRoberts, R.E., 2010. National Forest Inventories – Pathways for Common Reporting. Springer, Heidelberg.

van Leeuwen, M., Hilker, T., Coops, N.C., Frazer, G., Wulder, M.A., Newnham, G.J., Culvenor, D.S., 2011. Assessment of standing wood and fiber quality using ground and airborne laser scanning: a review. For. Ecol. Manage. 261, 1467–1478.

Xu, W., Su, Z., Feng, Z., Xu, H., Jiao, Y., Yan, F., 2013. Comparison of conventional measurement and LiDAR-based measurement for crown structures. Comput. Electron. Agricult. 98, 242–251. http://dx.doi.org/10.1016/j.compag.2013.08.015.

Zianis, D., Muukkonen, P., Mäkipää, R., Mencuccini, M., 2005. Biomass and stem volume equations for tree species in Europe. Silva Fennica Monogr. 4, 63.